Appl Biochem Biotechnol (2008) 149:9–22
DOI 10.1007/s12010-007-8124-9

Spectroscopic Characterization of Thiazole Orange-3 DNA Interaction

J. Ghasemi · Sh. Ahmadi · A. I. Ahmad · S. Ghobadi

Received: 3 June 2007 / Accepted: 6 December 2007 /
Published online: 9 February 2008

Abstract The interaction of a new derivative of thiazole orange (TO-3) with calf thymus DNA (ctDNA) has been investigated by fluorescence and absorption spectroscopy. When TO-3 binds to ctDNA, absorption bands exhibit significant hypochromicity at low base pair/dye ratio (BP/D ratio), and high BP/D show hyperchromicity with red shift. The spectral changes are attributed to the different species formed between TO-3 and ctDNA in the titration course of the dye molecule with DNA. Multivariate curve resolutions–alternating least squares (MCR–ALS) is applied to the absorption measurements recorded to recover the concentration profiles and the pure spectra of the DNA/TO-3 complexes involved in the process. The binding constant and size of the binding site have been determined spectrophotometrically using the McGhee von Hippel equation. MCR–ALS has been used to reveal the precise concentration profiles of all detectable species formed between ctDNA and TO-3 and their pure spectral profiles.

Keywords ctDNA · TO-3 · Fluorescence · Absorption spectra · MCR–ALS

Introduction

Cyanine dyes are known since 1856 [1] and the interest on this class of fluorescent molecules has been increasing recently [2, 3]. Actually, cyanines have found some applications in various areas of the most recent technologies, as for instance in laser materials [4], in optical disks [5], and in solar energy trapping [6]. However, the principal use of these dyes is in the

J. Ghasemi (✉) · S. Ahmadi
Department of Chemistry, Razi University, Kermanshah, Iran
e-mail: Jahan.ghasemi@gmail.com

A. I. Ahmad
Department of Chemical and Biological Engineering, Chalmers University of Technology, Gothenburg, Sweden

S. Ghobadi
Department of Biology, Razi University, Kermanshah, Iran

field of biomedicine where they are employed as anticancer agents [7, 8] and in biochemistry where they find application as polynucleotides probing and staining [9–12]. The last application being connected with the interesting properties of cyanines to sharply increase their fluorescence upon interaction with polynucleotides [13, 14].

Symmetric and asymmetric cyanine dyes are able to bind to DNA by intercalation [15–19] but groove binding is also possible [20–23]. Classical intercalators are planar aromatic ring systems such as acridines, anthracyclines, ethidium bromide, etc. [24]. In particular, the intercalative mode of interaction was clearly shown by NMR spectroscopy for the cyanine homodimeric dye TOTO [25]. Norden and Tjerneld [26] were the first to provide evidence for two binding geometries of a cyanine dye–DNA complex. Typical representatives of groove-binding molecules are cations with unfused aromatic rings such as netropsin, distamycin, and Hoechst 33258 [24]. Groove-binding mode of interaction was also shown in the case of the styrylcyanine dye DSMI [27]. Groove-binding molecules display significant specificity to A/T sequence unlike intercalators showing either no binding preference or slight G/C base pair preference. Such specificity may be explained by the fact that A/T and G/C sequences form interbase cavities which fit for intercalation in a similar manner but their grooves are structurally different [24].

A recent investigation on the intercalation mechanism of two cyanines containing the benzothiazolium residue into DNA [28] has shown that the binding process occurs according to a sequential three-step mechanism where the first step of the sequence is too fast to be analyzed in terms of kinetic constants and exhibits a binding constant much higher than expected on the basis of the electrostatic theory. This result indicates that in the first stage of the binding process, forces other than electrostatic are also at work. The electrostatic and nonelectrostatic interactions, which precede the intercalation steps, are generally considered to be the cause of an "external" complex formation. External complexes form easily at low polymer to dye concentration ratios and are stabilized principally by dye–dye interactions [29]. Under conditions where intercalation is operative, i.e., at high polymer to dye concentration ratios, a different kind of external binding is observed, as in the case of the above-cited DNA/cyanine system. A comparative study of the binding equilibria of structurally modified dyes to DNA [30] has demonstrated that the external binding is sensitive to salt effects, contrary to the intercalation. In addition, it has been shown that external binding occurs with a gain of entropy. These results suggest that this type of external binding largely involves hydrophobic groove interactions.

It is well known that most cyanine dyes form molecular aggregates in water solutions [31, 32]. In the aggregates with the 'card-pack' structure, transition dipole moments of which are perpendicular to the aggregate axis, in the terms of the molecular exciton model [33], the electron transition to the top of an exciton zone occurs, so the absorption spectrum of such aggregates (H-aggregates) is shifted hypsochromically relative to the monomer one. The aggregates of another type in which the transition dipole moment is parallel to the aggregate axis ('head-to-tail' structure), are called J-aggregates. These aggregates are characterized by a bathochromic shift of the absorption spectrum relative to a single molecule spectrum because the electronic transition to the bottom of the exciton zone is permitted [32, 33]. Thus, the spectral manifestation of aggregate formation in absorption spectra is determined by the aggregate structure. The cationic dyes, which are positively charged in water solution, can form aggregates on the negatively charged surfaces [31, 34] or macromolecules [35–37] easier than in solution. In [35] H-aggregates formed by the molecules of acridine orange on different polyanions, particularly on nucleic acids, were studied. It was shown in [26, 36, 37] that pseudoisocyanine (PIC) can form J-aggregates located in the DNA grooves.

Recently, Glazer and coworkers have synthesized and characterized a new series of dyes that form highly fluorescent complexes with DNA. Among these, is a homodimeric thiazole orange dye that has a high binding affinity for DNA, forming complexes that are stable under a variety of conditions [38–40]. The light-up probe, which consists of a thiazole orange (TO) linked to a peptide nucleic acid oligomer, hybridizes specifically to complementary nucleic acids. A recent analog of TO is 1-carboxydecyl-4-{3-[3-methyl-3H-benzothiazol-2-ylidene]-propenyl}-quinolinium (TO-3) iodide salt (Fig. 1). TO-3 differs from TO by having the aromatic systems joined by a propenyl instead of a methylene bond. This can potentially make TO-3 a better label than TO. In groove binding, the dye is held within the groove of the DNA where the close proximity of the dye to the walls of the groove allows for Van der Waal's forces and hydrogen bonding to stabilize the complex [64]. The higher binding affinity of TO-3 compared with TO is probably attributed to the extension of the π-system of interacted ligand and ability of hydrogen bonding, and consequently, possesses stronger interaction with the base pairs of the DNA at minor groove [35]. Like TO, TO-3 is expected to form dimer in solution. In this paper, we characterize the dimerization equilibrium of TO-3 by absorption titration [41] and chemometric analysis.

Multivariate curve resolution–alternating least squares (MCR–ALS) is applied to the absorption measurements recorded to recover the concentration profiles and the pure spectra

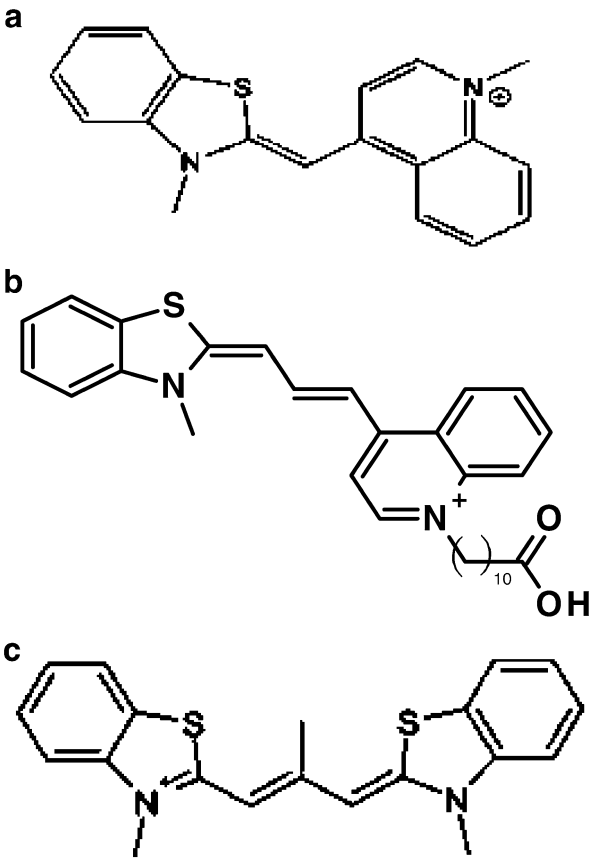

Fig. 1 Molecular structure of **a** TO, **b** TO-3, and **c** cyan 2

of the DNA complexes involved in the process [41–44]. The resolution results provide an interpretation of the mechanism of DNA/TO interaction. This method has allowed for the successful detection and modeling of intermediate conformations in similar processes induced by other agents and monitored with different techniques. This method has been applied for qualitative and quantitative description of protein folding, the mechanism of the process, and the evolution and nature of all protein conformations involved [45, 46].

Experimental

Materials

All the chemicals used were of analytical reagent grade. TO-3 was synthesized as described [47], and its purity was spectroscopically determined. A stock solution (3.1×10^{-3} M) was prepared by dissolving solid TO-3 in pure ethanol.

The high molecular weight DNA used in this study was extracted and purified from calf thymus by a standard proteinase K/phenol-chloroform extraction technique [48]. The DNA concentration was determined using an extinction coefficient of 6,600 $M^{-1}cm^{-1}$ at 260 nm and expressed in terms of base molarity [49]. DNA purity was determined by spectrophotometric measurement of absorbance ratio at A_{260}/A_{280} [50].

Methods

Fluorometric Measurements

The fluorometric measurements were carried out by a Cary Eclipse spectrofluorimeter. Fluorometric titrations of TO-3 were performed by adding small aliquots of a concentrated DNA solution to a TO-3 solution at 6×10^{-6} M in 0.01 M Tris buffer, pH=7.2. Samples were excited at 530 nm, and emission was scanned between 545 and 600 nm. All spectra were recorded at 25 °C.

Spectrophotometric Measurements

Absorption spectra were recorded with the CARY-100 Bio (Varian) UV–Vis spectrophotometer equipped with a temperature controller. Quartz cuvettes of 1 cm path length were used. Titrations of the TO-3 with DNA were performed by adding small aliquots of a concentrated DNA solution to a TO-3 solution at constant concentration. All solutions were equilibrated for at least 2 min before measuring emission profiles at 25 °C. MCR–ALS of the data was carried out through the MATLAB program MCR–ALS (http://www.ub.es/gesq/mcr/ntheory.htm) [51].

Data Treatment

Determination of Dimerization Constant of TO-3

The dimeric constant, concentration profiles for the monomer and dimer, and spectral responses of the monomer TO-3 and dimer TO-3 were determined by the DATAN package.

The thermodynamic parameters of the dimerization reaction of TO-3 were calculated from the dependence of dimeric constant on the temperature (van't Hoff equation) [52–54].

Multivariate Curve Resolution–Alternating Least Squares (MCR–ALS) on Absorbance Data

The absorption data have been modeled using MCR–ALS, which allows for the resolution of the concentration profiles and the pure spectra of the different species of a multicomponent chemical system [43].

The absorption spectra of DNA titrations with TO-3 were organized in a matrix **D** ($r \times c$) where the rows (r) are the absorption spectra collected at each concentration of DNA and the columns (c) describe the variation of the absorbance with increasing DNA concentration each wavelength. Bearing in mind that spectroscopic measurements follow the Lambert–Beer law and that the MCR–ALS method assumes that the experimental data follow a bilinear model, the matrix **D** can be decomposed into two matrices, **C** and $\mathbf{S}_T$, following the same model:

$$\mathbf{D} = \mathbf{C}\mathbf{S}_T + \mathbf{E} \tag{1}$$

where **C** contains the concentration profiles of the species in their columns and the rows of $\mathbf{S}_T$ show the pure spectra of these species. The **E** matrix represents the experimental error.

The MCR–ALS method resolves Eq. 1 following a series of steps. The first one is determination of the number of components, i.e., the number of complexes. A first estimation of the number of complexes is obtained from singular value decomposition (SVD) [55], although this number must be considered as an approximation and the definitive number of process contributions will be defined by the resolution results. The second step is construction of an initial estimate of either the **C** or the $\mathbf{S}_T$ matrix derived from chemometric methods, such as evolving factor analysis (EFA) [56, 57] or methods based on the selection of the purest variables [58, 59], or from the selection of representative spectra. Once the initial estimates are constructed, an iterative alternating least squares optimization of matrices **C** and $\mathbf{S}_T$ is carried out until convergence is achieved. Although MCR–ALS does not require any previous knowledge about the system, either chemical or mathematical, the addition of information helps to decrease the ambiguity in the final results. This information is obtained constraining the concentration profiles (**C**) and spectra ($\mathbf{S}_T$) during the iterative optimization. Constraints used in this study have been nonnegative in the absorption and concentration direction, and closure in the concentration direction [43]. Local rank, which imposes the absence or presence of some species in a specific ctDNA to dye concentration ratio (P/D), has been used to recover the concentration profiles. Such information comes from the application of local rank analysis methods, such as EFA [55–61].

The resolution process ends when the reproduced data matrix (**D***) obtained from the product of the resolved concentrations profiles (**C**) and spectra ($\mathbf{S}_T$) is similar enough to the original matrix **D**. Convergence is assumed to be fulfilled when the difference in fit between two consecutive iterations is less than 0.1%. The quality of the MCR–ALS model is assessed by the lack of fit, which is estimated by the equation:

$$\text{lack of fix} = 100 \times \sqrt{\frac{\sum \left(d_{ij}^{*} - d_{ij}\right)}{\sum d_{ij}^{2}}} \tag{2}$$

where d_{ij} is an element of the experimental matrix **D** and d_{ij} is the element of the MCR–ALS-reproduced matrix **D***.

Determination of Binding Constant of DNA and TO

The absorption spectral titration data have been analyzed using the McGhee–Von Hippel equation [62, 63] (Eq. 3) for cooperative binding model by nonlinear least squares analysis:

$$r/m = K_b(1-nr)\{(2w-1)(1-nr)+r-R/2(w-1)\times(1-nr)\}^{(n-1)} \times\{1-(n+1)r-R/2(1-nr)\}^2, \quad (3)$$

where r is the $[\text{complex}]_{\text{bound}}/[\text{DNA}]_{\text{tot}}$; m is the concentration of free complex; K_b is the binding constant; R is $\left[1-(n+1)r)^2+4wr(1-nr)\right]^{1/2}$; n, size of binding site, is the number of polynucleotide monomer units involved in the binding of one dye molecule under complete saturation conditions; and w is the cooperative parameter characterizing the interaction among neighborly bound TO-3 monomer and TO-3 aggregates, when its value is unity the process is noncooperative. The intrinsic binding constant K_b, n, and w were determined by this method.

Results and Discussion

TO Aggregation

It is known that cyanine dyes tend to self-aggregate [31, 32], and as this process can influence the course of dye binding to a given substrate, the feature of self-aggregation processes of TO-3 in the absence of DNA were investigated.

Figure 2a shows optical absorbance of TO-3 at various concentrations. TO-3 at 0.5 μM concentration exhibits a spectrum with two distinct maxima at 550 and 620 nm (Fig. 2b). With increasing concentration of TO-3, the shoulder at 504 nm develops into a peak. When the ratio of the absorbance values at 504 nm over the absorbance values at 550 nm was plotted vs TO-3, concentrations ranging from 0.5 to 27.8 μM, a nonlinear dependence, were observed, which indicates the presence of dimer and monomer (Fig. 2c). These results indicate the location the absorbance maxima for monomer were 620 and 550 nm whereas the dimeric form expresses an increased absorption at 504 nm.

The monomer–dimer equilibrium of TO-3 was investigated by means of UV–Vis spectroscopy. The data have been processed by a recently developed chemometric method for quantitative analysis of undefined mixtures, which is based on simultaneous resolution of the overlapping bands in the whole set of absorption.

The dimerization constant of TO-3 has been determined by studying the dependence of the absorption spectrum on temperature in the range 20–85 °C at 2.13×10^{-5} M total concentrations of dye. Figure 3b is the absorption spectra of TO-3 in aqueous solution recorded at 5 °C intervals from 20 to 85 °C. Utilizing the van't Hoff relation, which describes the dependence of the equilibrium constant on temperature, as constraint, we determine the spectral responses of the monomer and dimer species. Figure 3a indicates the spectra of monomer and dimer. By increasing the temperature, the absorption peaks around 550 and 620 nm grow and the shoulder around 504 nm decreases. At 509 nm, an isosbestic point is observed that indicates a specific wavelength at which two (or more) chemical species, likely monomers and dimers (H- and J-aggregates) have the same absorptivity [68]. The molar ratio of the TO-3 monomer and dimer and the temperature dependence of the dimerization constant have been indicated in Fig. 3c and d, respectively. As expected, K_D decreases with increasing temperature. From the dependence of $\ln(K_D)$ on $1/T$ (Fig. 3d), the

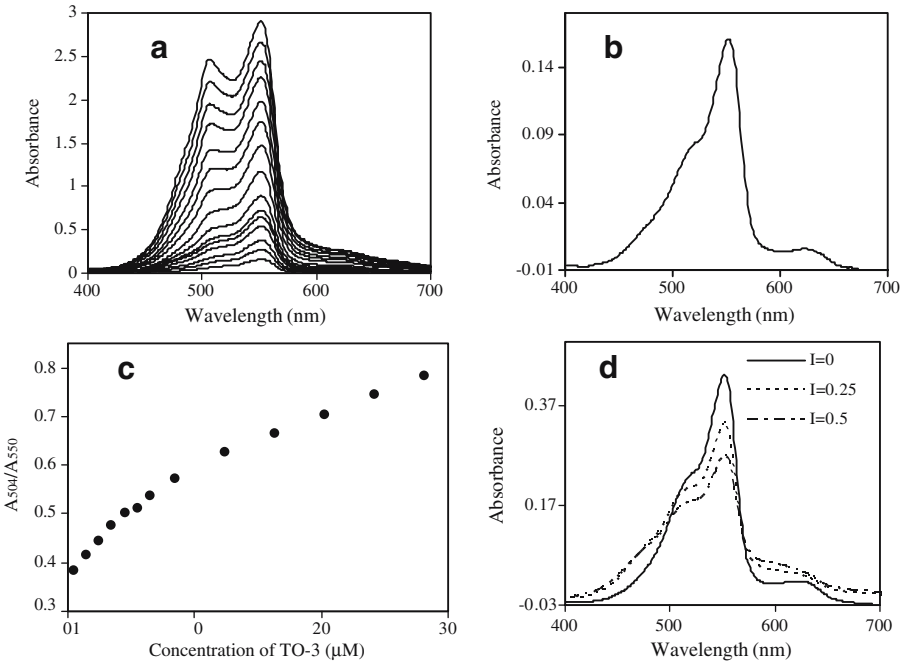

Fig. 2 **a** Absorbance spectra of TO-3 from 5.0×10^{-7} to 3.58×10^{-5}. **b** Absorbance spectra of TO-3 (5.0×10^{-7} M). **c** Relative absorbance of TO-3 at 504 nm compared to that at 550 nm as a function of the TO-3 concentration. **d** Absorption spectra of TO-3 aqueous solutions (3.0×10^{-6} M) with different amounts of NaCl

$\Delta H°$ and $\Delta S°$ values were determined. The $\Delta H°$ and $\Delta S°$ dimerization constants were obtained as 86.03 and −165.5 kJ/mol, respectively. The absorption spectrum of the TO-3 monomer has a maximum at 550 nm and a weak shoulder around 620 nm. It absorbs also in the UV region, having a maximum around 290 nm. The spectrum of the TO-3 dimer, as determined by chemometric analysis, has a maximum at 550 nm and a shoulder at 504 nm.

At low dye concentrations with just the dye monomers present, in the presence of NaCl, the initial absorption reduces and the spectra region broadens. The addition of NaCl along with a decrease in the monomer absorption induces a relative increase in the region of the H- and J-aggregates absorption (Fig. 2d). We think that in the presence of NaCl three dye species appear in the solution in equilibrium: the monomeric form, H-, and J-aggregates, characterized by the blue spectral shift and red spectral shift for H- and J-aggregates. Relative contents of these species depend on the NaCl and the dye concentrations.

DNA Binding Study

The equilibria of dye interaction with ctDNA were studied by both spectrofluorometric and spectrophotometric experiments. The fluorescence and absorption spectra display biphasic dependence. Fluorescence measurements and hole-burning studies of the thiazole orange derivatives TO-PRO-3 and TOTO-3 by Milanovich et al. [69] demonstrated that the dyes exhibit both types of interactions with double-stranded DNA, intercalation, and external binding.

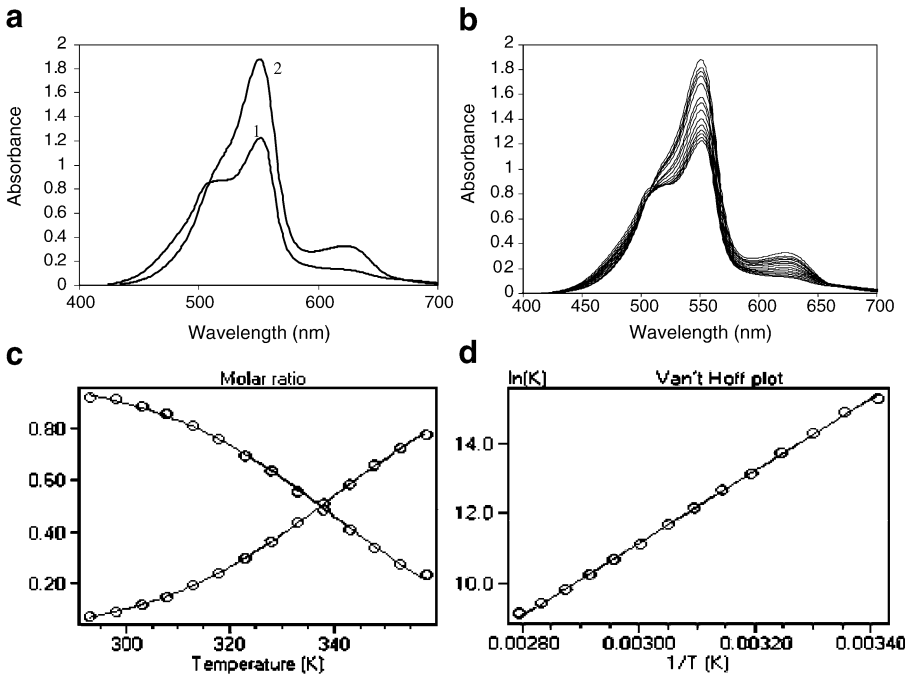

Fig. 3 **a** Absorption spectra of TO-3 monomer and dimer forms. **b** Absorption spectra of TO-3 (2.13×10^{-5} M) in aqueous solution recorded at 5 °C intervals from 20 to 85 °C. The absorbance increases with the increase of temperature. **c** Molar ratios of the TO-3 monomer (*1*) and dimer (*2*) forms. **d** Linear regression of $\ln(K_D)$ with respect to $1/T$

Fluorescence Studies

Figure 4 shows the effect of the addition of calf thymus DNA on the fluorescence spectrum of TO-3. The fluorescence spectra have the biphasic behavior. Initially, at low BP/D ratio, the addition of DNA quenches the fluorescence of the dye with λ_{max}=567 nm to approximately 75% along with the bathochromic shift of the emission spectra (BP/D< 0.65), and upon the addition of more DNA, a new emission peak at around 580 nm appears, which has enhanced strong fluorescence associated with the restricted rotation upon intercalation [47, 65], as reported previously by Milanovich et al. [69]. We may conclude that there are at least two modes of interactions. Therefore, the first branch of titration seems to instead represent an interaction of aggregates of TO-3 into the minor groove of DNA. In the second phase of titration (BP/D>0.65), when aliquots amounts of DNA are added, dye aggregation starts to dissociate, and finally, the TO-3 monomer intercalates into base pairs of DNA. Negligible fluorescence is seen for the bound TO-3 aggregations but the bound TO-3 monomer has intense fluorescence. This is most likely caused by stacking with the DNA bases, which locks the benzothiazole and the quinolinium rings in a plane, hindering the rotation around the interconnecting bond. This rotation is a channel for nonradiative relaxation from the excited state, and when restricted, TO-3 fluoresces. Clearly, the aggregates must be bound in a way that does not restrict rotation around the internal bond in at least one of the units. We speculate that this interaction with DNA by minor groove bonding is without restricted internal rotation.

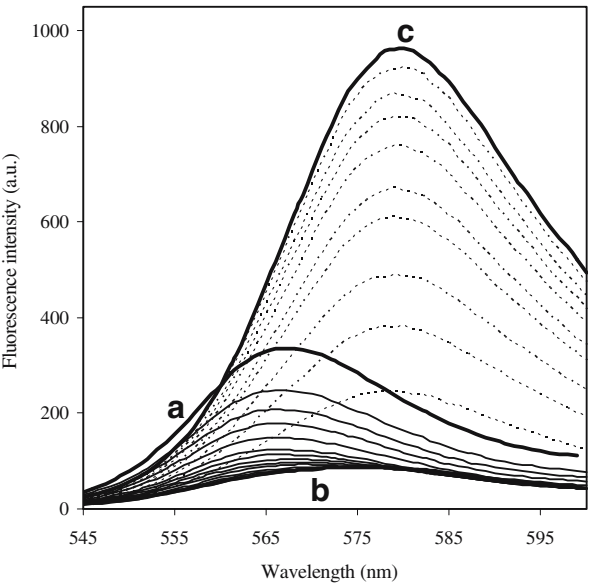

Fig. 4 Fluorescence spectra of the DNA/TO-3 system; 0.01 M Tris buffer, pH=7.2, T=25 °C. *a* [DNA]=0, [TO-3]=6.02×10^{-6} M; *b* [DNA]=7.67×10^{-6} M; *c* [DNA]=3.1×10^{-4} M. The excitation wavelength was 530 nm

Optical Absorption Studies

Optical absorption of TO-3 with different amounts of ctDNA indicates biphasic behavior (Fig. 5a). At low BP/D ratios, absorbance decreases without any important wavelength shift reaching the lowest level at BP/D ratio of around 0.65 and the effect saturates at this ratio (spectra a to b). This means that, even at very low DNA concentrations, all dye molecules are bound with DNA, thus demonstrating the high affinity of the dye toward DNA. At higher BP/D ratios (>0.65), absorbance changes show hyperchromicity along with red shift (spectra b to c).

Some absorbance spectra of TO-3 and DNA at different BP/D ratios were normalized for direct comparison (Fig. 5b). As the ratio of BP to AO increased from approximately 0 to 0.1, the absorbance peak near 504 nm (dimer peak) reduces. With continued additions of aliquots of DNA, in the BP/AO ratio 0.25, the absorbance peak reduces along with red and blue shift (aggregation) and the absorbance peak spreads. Upon increasing DNA concentration, the absorbance peak near 550 nm reduces and disappears at BP/D around 0.68. With the continued additions of aliquots of DNA and the subsequent increase in the BP/D ratio above 0.68, the absorbance at 550 nm begins to increase and display a red shift from 550 to 560 nm. This spectral peak at 560 nm gradually increased in height upon increasing DNA concentration before reaching an absorbance plateau at BP/D ratios of 1:885 and above; this spectrum is very similar to monomer TO-3 with 10 nm red shift. This may result from the dissociation of TO-3 aggregates in the presence of excess ctDNA. The 560 nm transition is assigned to the intercalated complex based on its small red shift relative to the unbound dye monomer (+10 nm) and on its prominence at low BP/D concentrations.

Salt Effect

It is known [66] that the ionic strength of the solution strongly affects the interaction of cyanine dyes with DNA, especially when this interaction occurs through a groove-binding mode [27]. An increase in the solution ionic strength leads to the degradation of aggregates

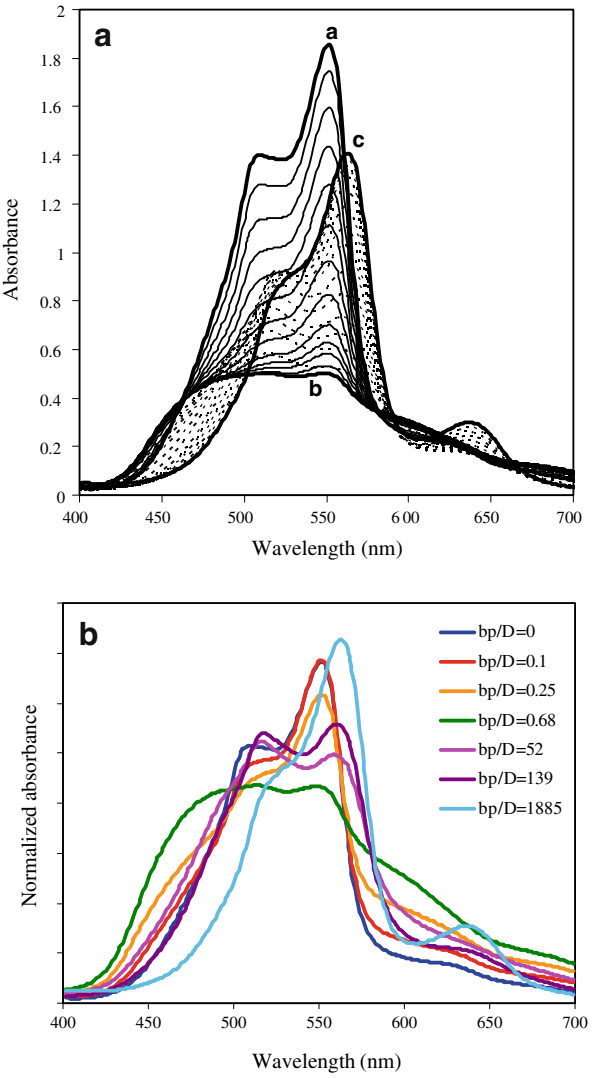

Fig. 5 **a** and **b** Absorbance spectra of the DNA/TO-3 system; 0.01 M Tris buffer, pH=7.2, T=25 °C. *a* [DNA]=0, [TO-3]=2.00×10^{-5} M; *b* [DNA]=2.72×10^{-5} M; *c* [DNA]=7.54×10^{-2} M

on DNA. On the other hand, as it was shown by Nygren et al. [66], the addition of salt or strong electrolytes to a solution releases the dye cations from the DNA grooves and causes the decrease in the amount of groove-binding cyanine dyes with DNA. In Fig. 6, the absorption spectra of the TO-3 solutions at constant concentration ([TO-3]=1.15×10^{-5} M) in the presence of DNA ([DNA]=3.45×10^{-5} M) and with different NaCl concentrations are shown. As one can see in Fig. 6, the addition of NaCl to the TO-3 solutions with DNA causes the decrease in aggregation band intensity and the increase in dimer band intensity. At higher NaCl concentration, 0.5 M, the aggregation bands become indistinguishable in the absorption spectrum. Thus, we believe that at this concentration of NaCl in the solution most of the dye molecules are released from DNA grooves and do not form aggregates in them.

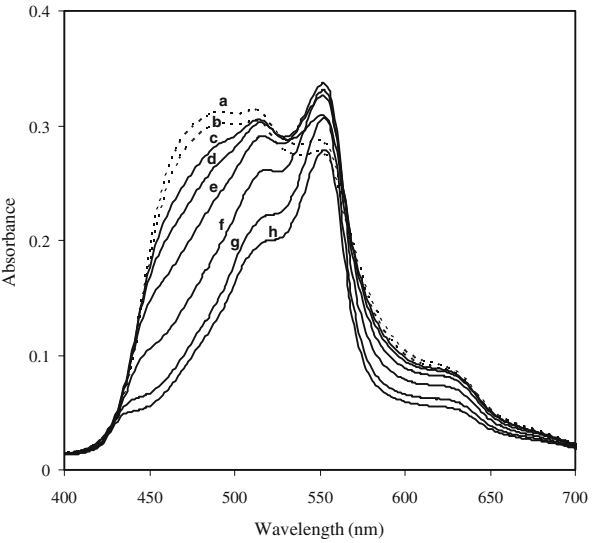

Fig. 6 Absorption spectra of the TO-3 buffer solutions at TO-3 (1.15×10^{-5} M) in the presence of DNA (3.45×10^{-5} M) with different amounts of NaCl (*a*, NaCl free; *b*, 0.01 M NaCl; *c*, 0.02 M NaCl; *d*, 0.03 M NaCl; *e*, 0.05 M NaCl; *f*, 0.1 M NaCl; *g*, 0.3 M NaCl; *h*, 0.5 M NaCl)

Resolution of the DNA/TO-3 Complexes

The application of SVD suggested the presence of three components in the data set. Using EFA initial estimates and applying the constraints mentioned in the data treatment section, the MCR–ALS results confirmed this hypothesis. Figure 7a and b shows the resolved spectra and concentration profiles of ctDNA/TO-3 complexes, respectively.

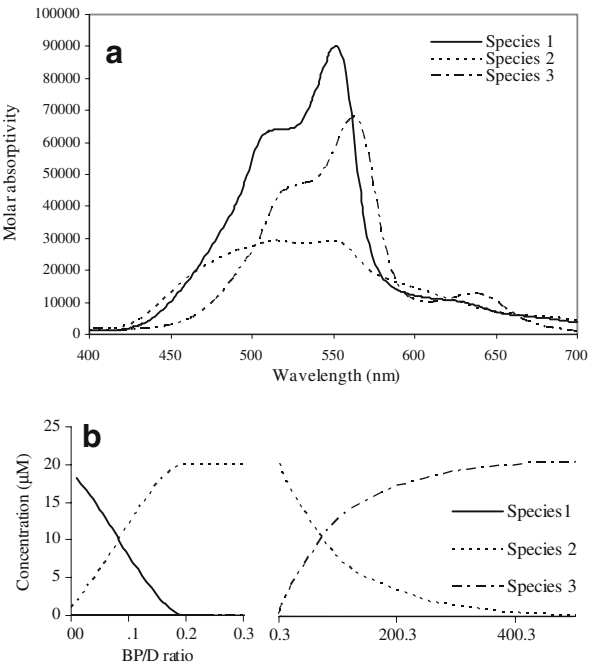

Fig. 7 MCR–ALS results of the DNA/TO-3 interactions. **a** Absorption spectra of species formed between DNA and TO-3. **b** Concentration of these species as a function of DNA concentration

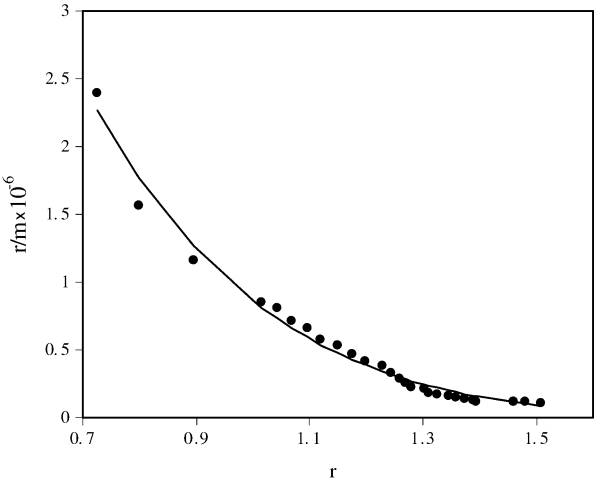

Fig. 8 Scatchard plot for the interaction of DNA with TO-3 ([TO-3]=2×10^{-5} M in 0.01 M Tris buffer, pH=7.2, T=25 °C)

Determination of the Binding Constant of ctDNA and TO-3

The absorption spectral titration data (for BP/D<0.65) have been analyzed using the McGhee–Von Hippel equation (Eq. 3) for the cooperative binding model by nonlinear least squares analysis. Absorbance Scatchard plot for the binding of TO-3 to ct is given in Fig. 8. The intrinsic binding constant K_b of 9.86×10^6 (n=0.37; w=1.59) determined for the TO-3 complex is higher than TO ($K_b=1.7\times10^5$ M^{-1}; n=2), benzothiazole orange ($K_b=3.9\times10^4$ M^{-1}; n=2.1) [65], and cyan 2 [66] ($K_b=1.5\times10^4$ M^{-1}; n=2) complexes. The value of w being higher than unity indicates that the DNA binding of TO-3 is cooperative. It can indicate the presence of TO-3 aggregates. TO-3 as well as complexes of groove-binding molecules, netropsin and distamycin A, stabilized by hydrogen bonds may have the K_b values as large as 10^8–10^9 M^{-1} [67].

Conclusions

We conclude that TO-3 binds both as monomers and as aggregates to ctDNA. Its interaction with ctDNA at rather low BP/D decreases the intensity of its absorption and its fluorescence quantum yield, as well. However, the aggregation reduces and finally disappears when the relative DNA concentration grows. Rather, high relative concentrations of DNA increase the intensity of its absorption and fluorescence. At low BP/D, TO-3 molecules aggregate and bind to DNA in the groove bindings. On the increase in the DNA concentration, TO-3 molecules bind to DNA in the monomeric form and mainly via intercalation that follows external complex formation. The increase in the solution ionic strength leads to the release of the dye molecules from the DNA grooves and aggregates are not formed in this case. The changes in the spectral pattern of the TO-3 because of the addition of the ctDNA molecules clearly showed the binding of the dye molecule to the DNA structure. MCR–ALS is applied to the absorption measurements recorded to recover the concentration profiles and the pure spectra of the DNA/TO complexes involved in the process. The binding constants and the size of the binding site of the ctDNA molecule have been determined. According to the linear dependence of absorption on the DNA concentration,

this TO derivative can be used as spectrophotometric probe in the determination of DNA concentrations.

References

1. Williams, C. H. G. (1856). *Transactions of the Royal Society of Edinburgh*, *21*, 377.
2. Armitage, B. A. (2005). *Topics in Current Chemistry*, *253*, 55.
3. Mishra, A., Behera, R. K., Behera, P. K., Mishra, B. K., & Behera, G. B. (2000). *Chemistry Reviews*, *100*, 1973.
4. Lanzafame, J. M., Muenter, A. A., & Brumbaugh, D. V. (1996). *Chemical Physics*, *210*, 79.
5. Spitler, M. T., Ehret, A., Kietzmann, R., & Willing, F. (1997). *Journal of Physical Chemistry B*, *101*, 2552.
6. Saito, K., & Yokoyama, H. (1994). *Thin Solid Films*, *243*, 526.
7. Kawakami, M., Koya, K., Ukai, T., Tatsuta, N., Ikegawa, A., Ogawa, K., et al. (1998). *Journal of Medicinal Chemistry*, *41*, 130.
8. Skripchenko, A., Wagner, S. J., Thompson-Montgomery, D., & Awatefe, H. (2006). *Transfusion*, *46*, 213.
9. Rye, H. S., Yue, S., Wemmer, D. E., Quesada, M. A., Haugland, R. P., Mathies, R. A., et al. (1992). *Nucleic Acids Research*, *20*, 2803.
10. Deligeorgiev, T. G. (1998). In S. Daehne, U. Resch-Genger, & O. S. Wolfbeis (Eds.) *Near-infrared dyes for high technology applications, NATO ASI series* p. 125. Dordrecht: Kluwer.
11. Hossain, M. Z., Ernst, L. A., & Nagy, J. I. (1995). *Neuroscience Letters*, *184*, 71.
12. Norman, D. G., Grainger, R. J., Uhrin, D., & Lilley, D. M. (2000). *Biochemistry*, *39*, 6317.
13. Goodwin, P. M., Johnson, M. E., Martin, J. C., Ambrose, W. P., Marrone, B. L., Jett, J. H., et al. (1993). *Nucleic Acids Research*, *21*, 803.
14. Guerrieri, S., Johnson, I. D., Bustamante, C., & Wells, K. S. (1997). *Analytical Biochemistry*, *249*, 44.
15. Netzel, T. L., Nafisi, K., Zhao, M., Lenhard, J. R., & Johnson, I. (1995). *Journal of Physical Chemistry*, *99*, 17936.
16. Larsson, A., Carlsson, C., & Jonsson, M. (1995). *Biopolymers*, *36*, 153.
17. Jarikote, D. V., Krebs, N., Tannert, S., Roeder, B., & Seitz, O. (2006). *Chemistry–A European Journal*, *13*, 300.
18. Karunakaran, V., Perez Lustres, J. L., Zhao, L., Ernsting, N. P., & Seitz, O. (2006). *Journal of the American Chemical Society*, *128*, 2954.
19. Karlsson, H. J., Mattias, H., Bergqvist, P. L., & Westman, G. (2004). *Bioorganic and Medicinal Chemistry*, *12*, 2369.
20. Kapuscinski, J., & Skoczylas, B. (1978). *Nucleic Acids Research*, *5*, 3775.
21. Jorgenson, K. F., Varshney, U., & van de Sande, J. H. (1988). *Journal of Biomolecular Structure and Dynamics*, *5*, 1005.
22. Karlsson, H. J., Eriksson, M., Perzon, E., Akerman, B., Lincoln, P., & Westman, G. (2003). *Nucleic Acids Research*, *31*, 6227.
23. Karlsson, H. J., Lincoln, P., & Westman, G. (2003). *Bioorganic and Medicinal Chemistry*, *11*, 1035.
24. Blackburn, G. M., & Gait, M. J. (Eds.) (1990). Nucleic acids in chemistry and biology. New York: IRL Press at Oxford University Press.
25. Spielmann, H., Wemmer, D., & Jacobsen, J. (1995). *Biochemistry*, *34*, 8542.
26. Norden, B., & Tjerneld, F. (1977). *Biophysical Chemistry*, *6*, 31.
27. Kumar, C., Turner, R., & Asuncion, E. (1993). *Journal of Photochemistry and Photobiology A, Chemistry*, *74*, 231.
28. Biver, T., De Biasi, A., Secco, F., Venturini, M., & Yarmoluk, S. (2005). *Biophysical Journal*, *89*, 374.
29. Biver, T., Ciatto, C., Secco, F., & Venturini, M. (2006). *Archives of Biochemistry and Biophysics*, *452*, 93.
30. Zimmermann, H. W. (1986). *Angewandte Chemie & Angewandte Chemie International Edition in English*, *25*, 115.
31. West, W., & Sandra, P. (1965). *Journal of Physical Chemistry*, *69*(6), 1894.
32. Kasha, M. (1963). *Radiation Research*, *20*, 55.
33. Herz, A. H. (1974). *Photographic Science and Engineering*, *18*(3), 323.
34. Jockusch, S., Turro, N. J., & Tomalia, D. A. (1995). *Macromolecules*, *28*, 7416.
35. Bradley, D. F., & Wolf, M. K. (1959). *Proceedings of the National Academy of Sciences of the United States of America*, *45*, 944.

36. Ogul'chansky, T. Yu., Yarmoluk, S. M., Yashchuk, V. M., & Losytskyy, M. Yu. (1999). In J. Greve, G. J. Puppels, & C. Otto (Eds.) *Spectroscopy of biological molecules: New directions* p. 309. Dordrecht: Kluwer.
37. Ogul'chansky, T. Yu., Losytskyy, M. Yu., Kovalska, V. B., Lukashov, S. S., Yashchuk, V. M., & Yarmoluk, S. M. (2001). *Spectrochimica Acta Part A*, *57*, 2705.
38. Rye, H. S., Yue, S., Wemmer, D. E., Quesada, M. A., Haugland, R. P., Mathies, R. A., et al. (1992). *Nucleic Acids Research*, *20*, 2803.
39. Benson, S. C., Mathies, R. A., & Glazer, A. N. (1993). *Nucleic Acids Research*, *21*, 5727.
40. Benson, S. C., Singh, P. S., & Glazer, A. N. (1993). *Nucleic Acids Research*, *21*, 5720.
41. Smilde, A. K., Tauler, R., Henshaw, J. M., Burgess, L. W., & Kowalski, B. R. (1994). *Analytical Chemistry*, *66*, 3345.
42. Tauler, R. (1995). *Chemometrics and Intelligent Laboratory Systems*, *30*, 133.
43. de Juan, A., Casassas, E., & Tauler, R (2000). Soft modeling of analytical data. In R. A. Meyers (Ed.) *Encyclopedia of Analytical Chemistry: Instrumentation and Applications* (p. 9800). New York: Wiley.
44. de Juan, A., & Tauler, R. (2003). *Analytica Chimica Acta*, *500*, 195.
45. Navea, S., de Juan, A., & Tauler, R. (2001). *Analytica Chimica Acta*, *446*, 185.
46. Borges, A., Tauler, R., & de Juan, A. (2005). *Analytica Chimica Acta*, *544*, 159.
47. Isacsson, J., & Westman, G. (2001). *Tetrahedron Letters*, *42*, 3207.
48. Sambrook, J., Fritsch, E. F., & Maniatis, T. (1989). *Molecular cloning. A laboratory manual*. New York: Cold Spring Harbour Press.
49. Aktipis, S., & Kindelis, A. (1973). *Biochemistry*, *12*, 1213.
50. Aaij, C., & Borst, P. (1972). *Biochimica et Biophysica Acta*, *269*, 192.
51. Jaumota, J., Gargalloa, R., de Juana, A., & Tauler, R. (2005). *Chemometrics and Intelligent Laboratory Systems*, *76*, 101.
52. Ghasemi, J., Niazi, A., Westman, G., & Kubista, M. (2004). *Talanta*, *62*, 835.
53. Kubista, M., Sjoback, R., & Nygren, J. (1995). *Analytica Chimica Acta*, *302*, 121.
54. Fisher, R., & MacKenzie, W. (1923). *Journal of Agricultural Sciences*, *13*, 311.
55. Navea, S., de Juan, A., & Tauler, R. (2003). *Analytical Chemistry*, *75*, 5592.
56. Golub, G. H., & Van Loan, C. F (1989). *Matrix Computations* (2nd ed.). Baltimore: John Hopkins University Press.
57. Maeder, M. (1987). *Analytical Chemistry*, *59*, 527.
58. Maeder, M., & Zuberbühler, A. D. (1986). *Analytica Chimica Acta*, *181*, 287.
59. Windig, W., & Guilment, J. (1991). *Analytical Chemistry*, *63*, 1425.
60. Sanchez, F. C., Toft, J., van den Bogaert, B., & Massart, D. L. (1996). *Analytical Chemistry*, *68*, 79.
61. de Juan, A., Navea, S., Diewok, J., & Tauler, R. (2004). *Chemometrics and Intelligent Laboratory Systems*, *70*, 11.
62. McGhee, J. D., & Von Hippel, P. H. (1974). *Journal of Molecular Biology*, *86*, 469.
63. Carlsson, C., Larsson, A., Jonsson, M., Albinsson, B., & Norden, B. (1994). *Journal of Physical Chemistry*, *98*, 10313.
64. Hilal, H., & Taylor, J. A. (2007). *Dyes and Pigments*, *75*, 483.
65. Kolesnikova, D. V., Zhuze, A. L., & Zasedatelev, A. S. (1998). *DNKSpecifichnye Nizkomolekulyarnye Soedineniya*. Moskow: MFTI In Russian.
66. Nygren, J., Svanvik, N., & Kubista, M. (1998). *Biopolymers*, *46*, 39.
67. Biver, T., Boggioni, A., Secco, F., Turriani, E., Venturini, M., & Yarmoluk, S. (2007). *Archives of Biochemistry and Biophysics*, *465*, 90.
68. Yarmoluk, S. M., Lukashov, S. S., Losytskyy, M. Yu., Akerman, B., & Kornyushyna, O. S. (2002). *Spectrochimica Acta Part A*, *58*, 3223.
69. Milanovich, N., Suh, M., Jankowiak, R., Small, G. J., & Hayes, J. M. (1996). *Journal of Physical Chemistry*, *100*, 9181.